International Symposium
On Turbulence and Shear Flow
Phenomena (TSFP-9)
June 30 - July 3, 2015 *Melbourne, Australia*

STATISTICS AND SCALING OF ADVERSE PRESSURE GRADIENT TURBULENT BOUNDARY LAYERS

Callum Atkinson, Vassili Kitsios, Abel-John Buchner
Laboratory For Turbulence Research in Aerospace and Combustion,
Department of Mechanical and Aerospace Engineering,
Monash University, Clayton 3800, AUSTRALIA.
callum.atkinson@monash.edu

Julio Soria
Laboratory For Turbulence Research in Aerospace and Combustion,
Department of Mechanical and Aerospace Engineering, Monash University, Clayton 3800, AUSTRALIA.
Department of Aeronautical Engineering, King Abdulaziz University,
Jeddah 21589, KINGDOM OF SAUDI ARABIA

ABSTRACT

Turbulent boundary layers in regions of strong adverse pressure gradient (APG) acting over a flat plates are investigated using a series of particle image velocimetry measurements. Experiments are performed in a large horizontal water tunnel with a flexible roof whose height can be adjusted in order to tailor the pressure distribution on the flat plate at the floor of the tunnel. In the present case an self-similar APG TBL is formed over a domain of 7 boundary layer thickness at a momentum thickness based Reynolds number ranging from $\mathrm{Re}_{\delta_2} = 2000$ to 3000. Profiles of mean velocity and Reynolds stress are presented normalised by a variety of velocity and length scales, all of which should provide the same collapse for a truly self-similar flow. Each scaling was found to provide a better collapse of some quantities with respect to the others but no single scaling is able to account for the variation in all quantities due to slight departures from self-similarity.

INTRODUCTION

Understanding the structure and dynamics of turbulent boundary layers (TBL) in regions of adverse pressure gradient (APG) and particularly as flow approaches separation is essential for the optimal design and control of flow over aircraft, submarines, boats, cars and turbine blades. As flows over planar and axisymmetric streamlined bodies pass from regions of favourable and zero pressure gradient (ZPG) to increasingly strong APGs, mean profiles and Reynolds stress profiles demonstrate significant changes to the structure of turbulent flows. Strong APGs correspond to large streamwise gradients in the inviscid outer velocity U_e at the top of the boundary layer such that $\mathrm{d}U_e/\mathrm{d}x \ll 0$, which for irrotational outer flow results in a mean wall-normal gradient in the streamwise velocity $\mathrm{d}U_e/\mathrm{d}y \ll 0$ and a secondary source of mean shear away from the wall. This additional shear not only contributes to the production of turbulent kinetic energy, but also raises questions about the existence of a ZPG like overlap region in APG flows.

As wall-bounded flows approach separation and the friction velocity $u_\tau \to 0$, the classic inner wall scaling of ZPG turbulent flows is undefined and the rational for this scaling no longer applies. The appropriate scaling for flows of spatial varying APG remains an open question, complicated by the influence of upstream conditions and flow history. Self-similar APG TBLs represent a 'simpler' case which we define as a flow in which each term in the Navier-Stokes equations have the same proportionality to streamwise position (x) (Castillo & George, 2001; Castillo & Wang, 2004). This requires the following parameter to remain constant and independent of x where:

$$\begin{aligned}\Lambda &= \delta_1 \frac{\partial P_e}{\partial x} \Big/ \left(\rho U_e^2 \frac{\partial \delta_1}{\partial x}\right) \\ &= (U_p/U_e)^2 \Big/ \frac{\partial \delta_1}{\partial x},\end{aligned} \tag{1}$$

where δ_1 is the displacement thickness, P_e is the pressure of the outer flow, and U_p is the pressure velocity defined in Mellor & Gibson (1966) as:

$$U_p = \left(\frac{\delta_1}{\rho}\frac{\partial P_e}{\partial x}\right)^{1/2}. \tag{2}$$

The condition of equation 1 represents a more general case of self-similar APG than that associated with requirement of a constant non-dimensional pressure gradient β as proposed by Clauser (1954), where:

$$\begin{aligned}\beta &= \delta_1 \frac{\partial P_e}{\partial x} \Big/ \tau_w \\ &= \delta_1 \frac{\partial P_e}{\partial x} \Big/ (1/2 c_f \rho U_e^2),\end{aligned} \tag{3}$$

τ_w is the shear stress at the wall and $c_f = 2\tau_w/\rho U_e^2$ is the local skin friction coefficient. For β to be constant and the

flow to be self-similar (i.e. Λ = constant) it follows from equations 1 and 3 that c_f and $\partial\delta_1/\partial x$ must share the same dependency on x and consequently:

$$c_f \propto \frac{\partial \delta_1}{\partial x}. \tag{4}$$

Given that in an APG the displacement thickness will grow as the skin friction decreases, equation 4 can only be satisfied if c_f and $\partial\delta_1/\partial x$ are both constant, which in the case of constant β self-similar APG results in a linear variation in δ, δ_1 and δ_2 with x, where δ is the boundary layer thickness and δ_2 is the momentum thickness, as well as a constant U_p/U_e, c_f and shape factor $H = \delta_1/\delta_2$.

Numerous attempts have been made to determine the appropriate length and velocity scales for self-similar APGs. For the more general self-similar flow as detailed in the accompanying paper of Kitsios *et al.* (2015), analysis of the governing equations indicates that self-similar profiles should collapse under a velocity and lengths scale:

$$U_o = KU_e \tag{5}$$
$$L_o = \delta_1/K, \tag{6}$$

where K is an arbitrary constant.

For the special case of self-similar APGs with constant β Mellor & Gibson (1966) show that velocity deficit profiles collapse for a given β using the pressure velocity as the velocity scale and a length scale defined as:

$$U_o = U_p \tag{7}$$
$$L_o = \delta_1 U_e/U_p. \tag{8}$$

If we recall that in this case U_p/U_e must be constant, this scaling consequent reduces to the general scaling where $K = U_p/U_e$. Unfortunately U_p is only defined when $dP/dx > 0$ and like u_τ scaling cannot be applied over the full range of possible pressure gradients.

Zagarola & Smits (1998) introduce a separate scaling that as in the general solution can be defined across a full range of pressure gradients by enabling the constant K to be represented by the ratio of the displacement and boundary layer thickness $K = \delta_1/\delta$ with the velocity and length scales taking the form:

$$U_o = U_e \frac{\delta_1}{\delta} \tag{9}$$
$$L_o = \delta_1/(\delta_1/\delta) = \delta. \tag{10}$$

As with the U_p scaling the above scaling reduces to the general scaling in a self-similar flow with constant β as δ and δ_1 both vary linearly with x, their ratio remaining constant and as in the case of each of the aforementioned scalings should collapse all self-similar profiles for a given Λ and β. In the case of the scaling of Zagarola & Smits (1998) the ratio δ_1/δ attempts to represent that change in the shape of the mean velocity profile that associated with changes in pressure gradient, suggesting this scaling may extend to regions where flow is not self-similar.

Analysis of self-similar APG TBLs over a flat plate has the ability to provide important details about the influence of local pressure gradient on the structure and dynamics of these turbulent flows, free from the contamination of upstream flow history or surface curvature that typically accompany the measurement of spatially varying APG flows. In practice the formation of such a self-similar APG TBL is non-trivial owing to the coupling of the free stream pressure gradient with boundary layer entrainment and tunnel cross-sectional area, consequently little experimental data exists in which a large self-similar domain is present. Skåre & Krogstad (1994) performed a series of hot-wire measurements in a wind-tunnel with a deformable roof enabling the formation of a strong APG TBL with a nominally constant β, H, c_f and linearly increasing δ, δ_1 and δ_2 over a domain of approximately 5δ with $\beta \approx 20$ and $\mathrm{Re}_{\delta_2} = 39120$ to 50980. Skåre & Krogstad (1994) present some scatter between the mean velocity and Reynolds stress profiles when normalised by the estimated local friction velocity u_τ but do not quantify the collapse of any of these profiles under any of the proposed velocity scaling discussed above. Direct numerical simulations (DNS) of APGs have mostly been limited to non-self-similar APG cases such as that of Gungor *et al.* (2012), with the exception of the low Reynolds number APG cases of Lee & Sung (2008) and the recent moderate Reynolds number self-similar DNS of Kitsios *et al.* (2015).

In this paper we detail the results from experimental measurements of a strong APG TBLs on a flat surface approaching self-similarity. Details of the boundary layer profiles are presented along with wall-normal profiles of mean velocity and Reynolds stresses. The degree to which the previously mentioned scalings are able to collapse the data in and around regions of apparent self-similarity are assessed.

EXPERIMENTAL DATABASE

To generate APG TBLs over a flat surface, the 500 $\times$ 500 mm cross-section water tunnel at the Laboratory for Turbulence Research in Aerospace and Combustion (LTRAC) was modified to contract the flow below the water line of the tunnel via the addition of a secondary contraction, followed by a five metre long flexible polycarbonate roof (see figure 1). Spanwise members are affixed to the roof with threaded rods on each side of the member to allow the adjustment of the roof height at 19 individual stations downstream of the contraction. A large honeycomb with tubes of 15 mm diameter and equipped with a 2 mm $\times$ 2 mm wire mesh on each end was placed at the outlet of the fixed tunnel contraction in order to reduce the influence of the asymmetry of the contract on the flow downstream. A false floor with a half ellipse leading edge was placed at the very beginning of the first test-section (defined as x = 0 mm) with a TBL forming on the upper surface of the false floor. The height above the wall in the wall-normal direction is defined as y with the instantaneous velocity in the free-stream direction x represented by $U = \overline{u} + u$ where $\overline{u}$ is the mean velocity and u the fluctuating component. Each test-section is 1.1 m long. The false floor was installed to enable the future introduction of flow control mechanisms from beneath the floor. The use of a water tunnel rather than a wind tunnel leads to much longer time scales in the flow, which will enable time-resolved measurements using existing high-repetition rate lasers and high-speed cameras operating at $\approx$ 1 kHz. The roof downstream of the secondary

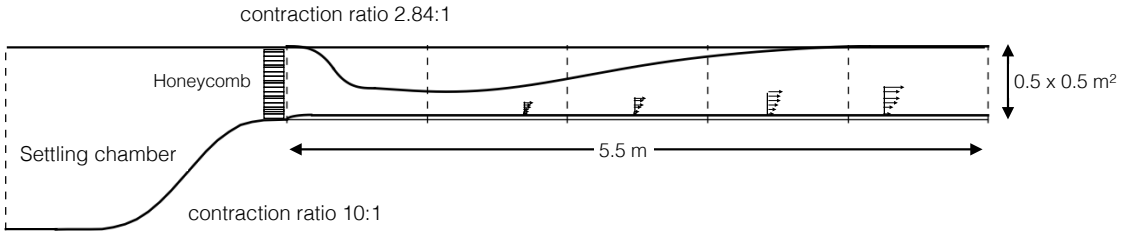

Figure 1. Schematic of the modified LTRAC water tunnel with fixed vertical contraction in the first test section, flexible roof and false floor along the tunnel length.

contraction was set with an angle of approximately 10 degrees over the majority of the second test-section, reducing to an almost level roof surface at the end of the third section.

The set roof height (h), measured boundary layer thicknesses (δ, δ_1, δ_2), free-stream velocity at the top of the boundary layer (U_e) and free-stream streamwise pressure gradient at the top of the boundary layer ($\partial P_e/\partial x$) are presented in figure 2. In strong APGs the mean streamwise velocity is not constant above the boundary layer as in ZPG TBLs, but rather increases through the boundary layer before decreasing with further height above the boundary layer where $\partial\overline{u}/\partial x < 0$. In the present paper U_e is therefore defined as the peak in the mean velocity profile $\overline{u}(y)$ with the boundary layer thickness δ defined as the turning point in the profile where $\overline{u}(\delta) = U_e$. This non-constant velocity above the TBL also influence the definition of the displacement and momentum thickness which can no longer be integrated to $y \to \infty$ but rather:

$$\delta_1 = \int_0^\delta \left(1 - \frac{\overline{u}(y)}{U_e}\right) \mathrm{d}y, \text{ and} \tag{11}$$

$$\delta_2 = \int_0^\delta \frac{\overline{u}(y)}{U_e}\left(1 - \frac{\overline{u}(y)}{U_e}\right) \mathrm{d}y. \tag{12}$$

The pressure gradient $\partial P_e/\partial x$ at $y = \delta$ was determined from the velocity gradient along the streamline at the top of the TBL via Bernoulli's equation.

Measurement of the velocity profiles at different stations along the tunnel were performed using an in-house multi-grid planar particle image velocimetry (PIV) algorithm (Soria, 1996) with a final size of 64×16 pixels, elongated in the streamwise direction. Images were acquired using a sCMOS camera with an array size trimmed to 1161×2560 pixels equipped with a 50 mm focal length Zeiss Makro-Planar lens with f-stop set to $f_\# = 2.8$ resulting in a spatial resolution of 19.2 pixels/mm and a lens magnification of $M = 0.124$. This corresponds to a field of view of $1.2\delta \times 2.6\delta$. Profiles presented were calculated from 4000 velocity fields record at a rate of 10 Hz and additionally averaged over a streamwise distance of 1.2δ. The flow was seeded with 11 μm Potters hollow glass spheres with a specific gravity $\gamma = 1.1$, resulting in lens diffraction limited particle image diameter of approximately 1 pixel. Illumination was provided by a dual cavity New Wave Gemini 100 mJ Nd:YAG laser, formed into a 1 mm thick light sheet with an estimated depth of field of 1.7 mm for the PIV images. The water temperature was 21.5 deg. C with a corresponding density $\rho = 997$ kg/m^3 and kinematic viscosity $\nu = 9.45 \times 10^{-7}$ m^2/s. The tunnel was run at constant motor speed of 15 Hz, corresponding to a free-stream speed of $U_e = 214$ mm/s in the absence of the added false floor and contraction.

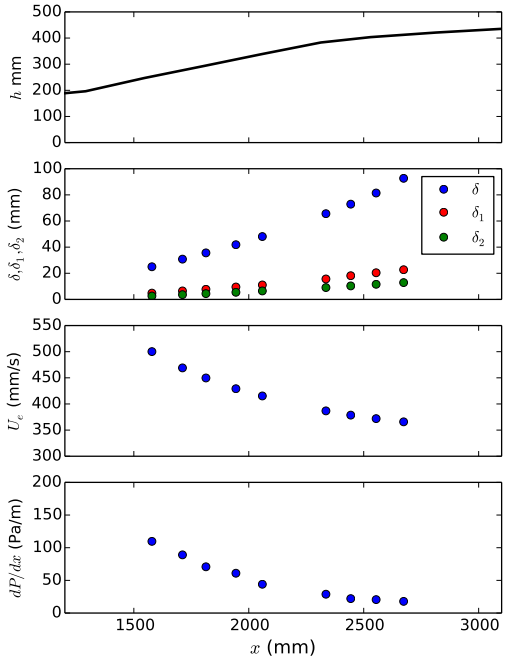

Figure 2. Roof height h, boundary layer thickness δ, displacement thickness δ_1, momentum thickness δ_2, measured free-stream velocity U_e and streamwise pressure gradient $\partial P_e/\partial x$.

RESULTS

The mean streamwise velocity profiles associated with each of the measured profiles are shown in figure 3 with x values for each plot indicating the location of the measurement relative to the start of the false floor. Figure 3 clearly shows the peak velocity at δ, while indicating a potential logarithmic region for each case, however higher resolution measurement near the wall are required to confirm this and enable an estimate of the local friction velocity u_τ.

From figure 2 the boundary layer thickness parameters δ, δ_1 and δ_2 all appear to be vary linearly for $1712 < x < 2059$ mm and $2336 < x < 2554$ mm as would be the case for regions of constant β and constant Λ. It can be shown by rearranging and integrating the expression in equation 1

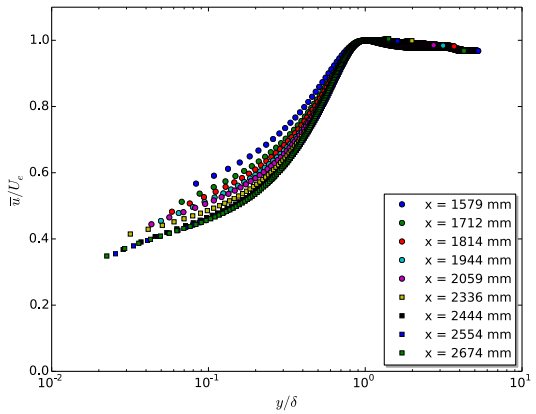

Figure 3. Wall-normal profile of mean streamwise velocity $\overline{u}(y)$ normalised by outer velocity and length scales.

that the velocity U_e must be related to the δ_1 by:

$$U_e = A\delta_1^{-\Lambda}, \tag{13}$$

where A is a constant of integration. It follows that Λ can therefore be determined from the gradient of the natural log of U_e against the natural log of δ_1 as shown in figure 4. The value of $\Lambda = -0.228$ is close to the expected value of $\Lambda = -0.23$ for the incipient self-similar APG TBL at the verge of separation. For a self-similar flow at the verge of separation $c_f \to 0$ results in a constant c_f which following equation 4, 1 and 3 results in a constant U_p/U_e, β and H.

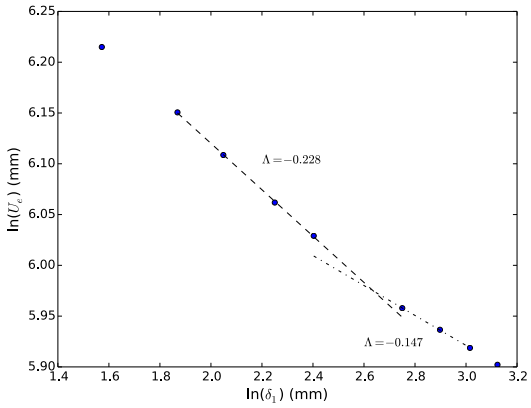

Figure 4. Logarithm of outer velocity U_e verses the logarithm of the displacement thickness δ_1. Dashed lines represent linear fits to obtain local values of Λ.

Figure 5 indicates a relatively constant H and U_p/U_e over almost the entire measurement range. The value of Λ computed at each location from equation 1 shows greater variation, in this case due to the variations in the local streamwise gradient of δ_1. The dashed lines in figure 5 represent the expected values of H and U_p/U_e for the incipient case (Mellor & Gibson, 1966) indicating that despite $\Lambda \to -0.23$ the pressures gradients are still lower than that which would be required to achieve the incipient case. The value of β cannot be determined from the present data without an estimation of u_τ which can only be made by using Clauser's method, which assumes that the logarithmic overlap region from ZPG flows is still valid in the strong APG case.

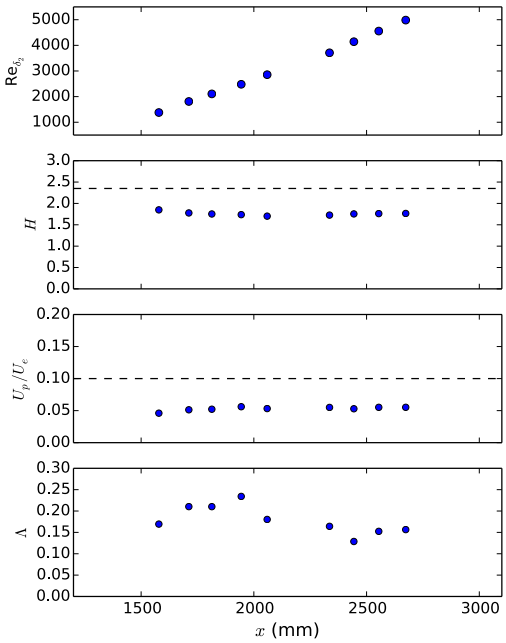

Figure 5. Momentum thickness based Reynolds number Re_{δ_2}, shape factor H, U_p/U_e and Λ.

A comparison of the present velocity deficit profiles to those computed by Mellor & Gibson (1966) for self-similar profiles with different values of constant β show that the profile and shape factor of the data in the range $1712 < x < 2059$ mm is consistent with a $\beta \approx 4$ as shown in figure 6. The velocity scale U_p and length scale $\delta_1 U_e/U_p$ provide a reasonable collapse of mean velocity and Reynolds stress profiles, both of which compare favourably with the DNS results of Kitsios *et al.* (2015). DNS results for similar β show a secondary peak in $< u.u >$ closer to the wall at $y^+ \approx 14$ the upper portion of which is just captured by the lower portion of the present experimental field of view. Current results indicate a better collapse of the wall normal stress than the streamwise. The lack of collapse may in part be due to the uncertainty associated in the estimation of δ_1 due to the lack of data near the wall. In the present case the calculation of δ_1 and δ_2 were performed assuming a linear velocity distribution from the lowest point of the measurement down to the wall, rather than assuming a particular near wall model.

Figure 8 shows the mean velocity and Reynolds stress profiles under the scaling suggested by the more general self-similar form, with the constant $K = 1$ resulting in a velocity scale U_e and length scale δ_1. Interestingly the relative collapse for $\overline{u}$ and $< v.v >$ is not as good as that observed for U_p scaling in figure 6 with the exception of $< u.u >$.

The scaling of Zagarola & Smits (1998) provides the best collapse of the mean velocity profile by accounting for change in the non-constant ratio of δ_1/δ for non-self-similar flows. An excellent collapse in the wall-normal

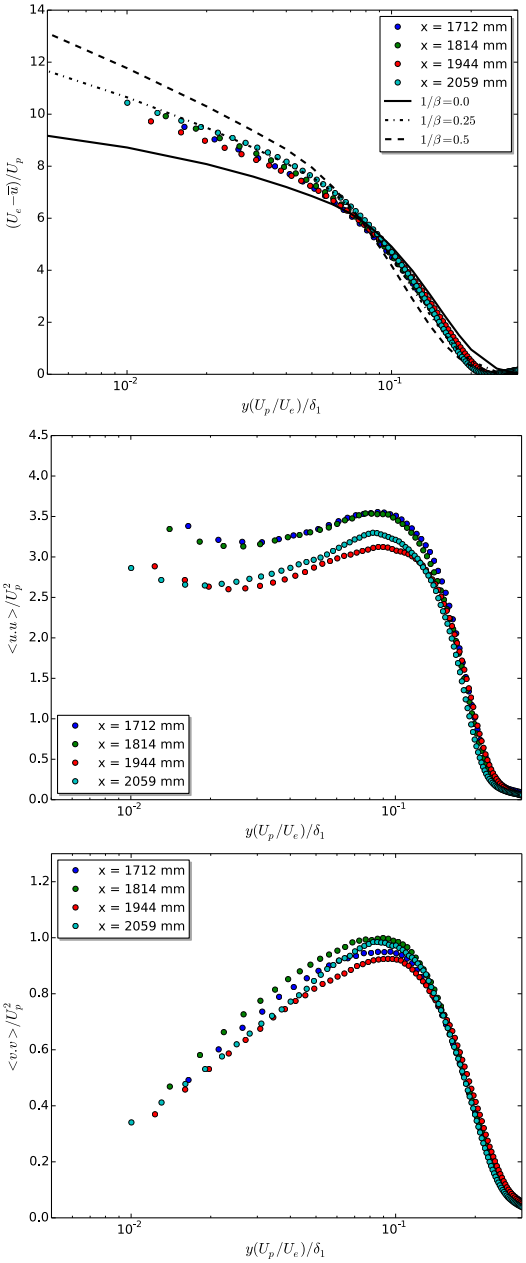

Figure 6. Mean streamwise velocity $\overline{u}$, streamwise $< u.u >$ and wall normal $< v.v >$ Reynolds stress profiles, normalised by the pressure velocity. Profiles associated with analytical solution of Mellor & Gibson (1966) for self-similar APG TBLs with constant β are shown for comparison. For clarity only every third data point is shown.

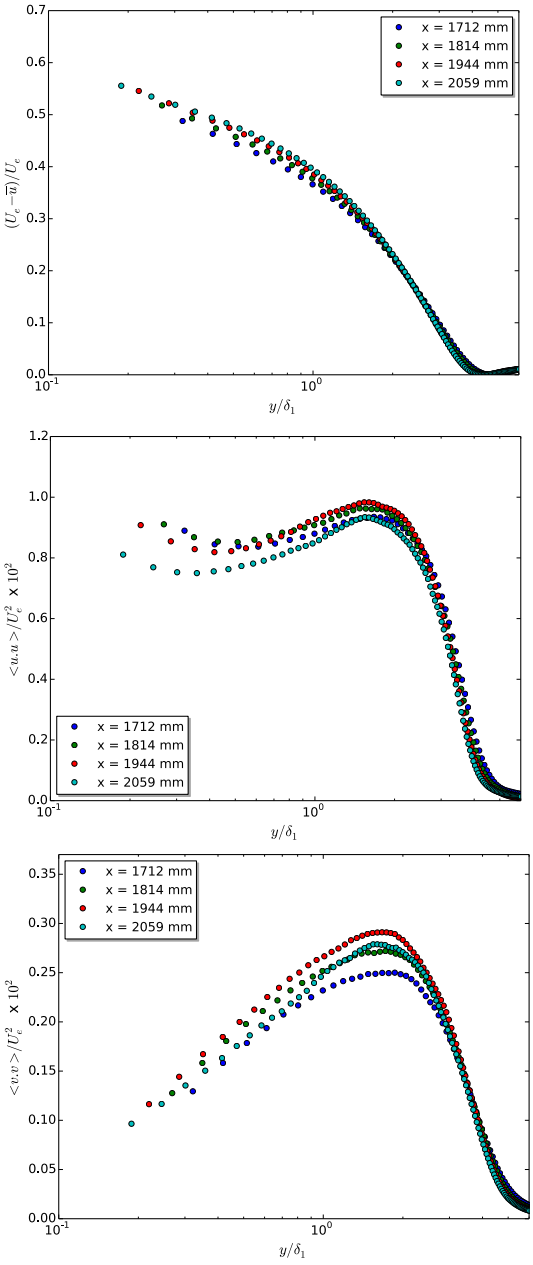

Figure 7. Mean streamwise velocity $\overline{u}$, streamwise $< u.u >$ and wall normal $< v.v >$ Reynolds stress profiles, normalised by the general self-similar APG scaling. For clarity only every third data point is shown.

stresses $< v.v >$ is also observed with the exception of the final profile, however this scaling provides the worst collapse of the streamwise stress $< u.u >$, particular approaching the wall. The degradation of the collapse of $< u.u >$ near the wall appears to be associated with the presence of the near wall peak, suggesting a dependence on u_τ or Reynolds number which is not present in any of the above scalings.

CONCLUDING REMARKS

Experimental measurements of adverse pressure gradient turbulent boundary layers are presented over a flat plate with an imposed strongly adverse pressure gradient. A region with near linear boundary layer growth and approximately constant shape factor was generated over a distance of approximately 7δ, parameters which have generally been taken as indicators of a self-similar APG with constant β. Attempts to collapse the mean velocity and Reynolds stress profiles over this region were not completely successful, suggesting that these parameters are not a sufficient test for self-similarity. It is not clear if this lack of collapse is due to

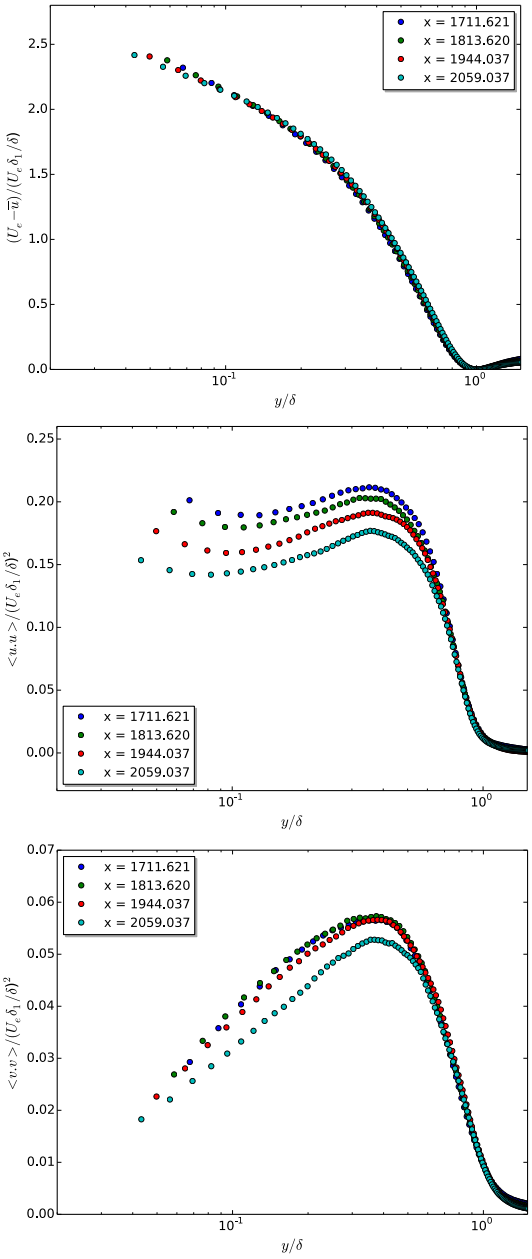

Figure 8. Mean streamwise velocity $\overline{u}$, streamwise $< u.u >$ and wall normal $< v.v >$ Reynolds stress profiles, normalised following the scaling of Zagarola & Smits (1998). For clarity only every third data point is shown.

the absence of self-similar flow or the experimental uncertainty associated with the estimation of the scaling parameters. A number of different velocity and length scales were considered, all of which should provide the same collapse for a self-similar flow with constant Λ and β. No one scaling provides an optimal collapse of all quantities. The scaling of Zagarola & Smits (1998) provides the best collapse of mean profiles and $< v.v >$, yet provides the worst collapse of $< u.u >$, failing to capture the magnitude of both the inner and outer peaks. Results suggest values of the more general self-similarity parameter Λ are more sensitive to departure from self-similarity than either the shape factor H or the streamwise gradients of δ, δ_1 and δ_2 indicating constant Λ may be a more reliable measure of self-similarity.

ACKNOWLEDGEMENT

The authors acknowledge the research funding from the Australian Research Council. Julio Soria gratefully acknowledges the support of an Australian Research Council Discovery Outstanding Researcher Award fellowship.

REFERENCES

Castillo, L. & George, W.K. 2001 Similarity analysis for turbulent boundary layer with pressure gradient: outer flow. *AIAA journal* **39** (1), 41–47.

Castillo, L. & Wang, X. 2004 Similarity analysis for nonequilibrium turbulent boundary layers*. *Journal of fluids engineering* **126** (5), 827–834.

Clauser, F. 1954 Turbulent boundary layers in adverse pressure gradients. *J. Aero. Sci.* **21**, 91–108.

Gungor, Ayse G, Simens, Mark P & JimÃŠnez, Javier 2012 Direct numerical simulations of wake-perturbed separated boundary layers. *Journal of Turbomachinery* **134** (6), 061024.

Kitsios, V, Atkinson, C., Sillero, J.A., Borrell, G., Jiménez, J., Gungor, A.G. & Soria, J. 2015 Direct numerical simulation of a self-similar adverse pressure gradient turbulent boundary layer. In *9th. Symp. on Turbulence and Shear Flow Phenomena (TSFP-9)*. The University of Melbourne, Australia, June 30- July 3.

Lee, Joung-Ho & Sung, Hyung Jin 2008 Effects of an adverse pressure gradient on a turbulent boundary layer. *International Journal of Heat and Fluid Flow* **29** (3), 568–578.

Mellor, GL & Gibson, DM 1966 Equilibrium turbulent boundary layers. *Journal of Fluid Mechanics* **24** (02), 225–253.

Skåre, Per Egil & Krogstad, Per-åge 1994 A turbulent equilibrium boundary layer near separation. *Journal of Fluid Mechanics* **272**, 319–348.

Soria, J. 1996 An investigation of the near wake of a circular cylinder using a video-based digital cross-correlation particle image velocimetry technique. *Experimental Thermal Fluid Science* **12**, 221–233.

Zagarola, Mark V & Smits, Alexander J 1998 Mean-flow scaling of turbulent pipe flow. *Journal of Fluid Mechanics* **373**, 33–79.